

Empirically Determined Wave Function for the Relaxed-Excited State of the F Center in KI^\dagger

L. F. Mollenauer* and G. Baldacchini†

Department of Physics, University of California, Berkeley, California 94720

(Received 26 June 1972)

A well-defined probability density has been extracted from measured hyperfine frequencies; it corresponds to a pure $|2p\rangle$ state peaking at a radius of 6.84 Å. The associated wave function is of a dynamic Jahn-Teller type, such that the orbitals $|x+iy\rangle$, $|x-iy\rangle$, and $|z\rangle$ are equally represented. The radiative lifetime calculated from this state agrees well with the experimentally measured one. The probability density also correctly predicts the known resonance linewidths in KI, KBr, and possibly KCl.

In a recent series of experiments, both the electron-spin-resonance (ESR) and electron-nuclear double-spin-resonance spectra (ENDOR) have been measured for the relaxed-excited state (RES) of the F center in KI.¹⁻³ We wish to report here the experimentally measured effect on these spectra of rotating the crystal axes with respect to the direction of the externally applied magnetic field, and to reveal the well-defined electronic probability density implied by these measurements.

The experimental facts may be summarized as follows: (1) The ESR g factor ($g=1.629$) is isotropic. (2) The ESR line shape is also isotropic and is Gaussian with a width at half-power points $\Delta H = 575 \pm 10$ Oe.³ (3) The ENDOR spectrum consists of approximately a dozen lines in the range $21 \text{ MHz} \leq \nu_E \leq 33.5 \text{ MHz}$.^{2,3} From the rate and direction of tuning with the magnetic field,³ it is known that all lines correspond to interactions with the halogen nuclei (I^{127} ; $I = \frac{5}{2}$; 100% natural abundance), and that they represent sum frequencies; i.e., $\nu_E = \nu_{hf} + \nu_Z$, where the nuclear Zeeman frequency, $\nu_Z = 18.50$ MHz for the field used. Thus, there is a well-defined maximum hyperfine frequency $(\nu_{hf})_{\max} = 15$ MHz. (4) In general, spacing of the ENDOR lines decreases monotonically with decreasing frequency, and, for $\nu_{hf} \lesssim 3$ MHz, the spectrum consists essentially of a continuum. (5) Rotation of the crystal axes with respect to the applied magnetic field produces no measurable shift or splitting of the ENDOR lines.

Isotropy of the g factor implies that the system cannot be properly described by a *static* Jahn-Teller effect. However, the basis for a proper dynamic treatment has been outlined in a recent Letter by Ham.⁴ According to Ref. 4, the wave function will be in the form of a sum of products of vibronic states with electronic states; furthermore, the solutions hinted at there suggest that the appropriate function, whatever its detailed

nature, will contain equal amounts of the electronic orbitals $|x+iy\rangle$, $|x-iy\rangle$, and $|z\rangle$. Thus, when we integrate over the vibronic coordinates to obtain a probability density in the reduced space of the electronic coordinates, cross terms between the various p orbitals will drop out by virtue of the orthogonality of the vibronic states. The resultant electronic density will then contain only a sum of (equal amounts of) squares of the three spherical harmonics, and will hence have no angular dependence. The reduced probability density is appropriate to the calculation of hyperfine interactions. Its use corresponds physically to the assumption that the vibrations average the electronic part of the wave function equally over all three p orbitals in a time short compared to one precessional period of the nucleus.

In the region outside the first shell of ions, the potential $V(\vec{r})$, when averaged over a sufficiently large space, can be approximated by a simple Coulomb term.⁵ We therefore choose simple single-electron atom $|2p\rangle$ states for the electronic part of the envelope function; i.e., these states have the radial dependence $\psi \propto \rho \exp(-\eta\rho)$, where ρ is the radial electron coordinate in units of the nearest-neighbor distance d ($d = 3.525$ Å for KI), and where η is an adjustable parameter. The reduced probability density then has the form

$$P_p(\rho) = (\eta^3/3\pi)(\eta\rho)^2 \exp(-2\eta\rho). \quad (1)$$

The above has been normalized such that $P(\rho)$ refers to a unit volume of d^3 .

Independence of the ENDOR spectrum from crystal orientation implies that anisotropic terms in the hyperfine interaction are negligible. Hence, only the isotropic contact term is important; as is well known, one may write

$$(\nu_{hf})_i = C_1 A P(\rho_i), \quad (2)$$

where A is the so called "amplification factor" that relates the actual probability density at the

site of the i th nucleus to $P(\rho_i)$ of the envelope function, and where C_1 is calculated in the standard way⁶ to have the numerical value $C_1 = 1.513d^3$ MHz for I^{127} nuclei in contact with the RES wave function. (C_1 for K nuclei is ~ 40 times smaller; hence interaction with K will be neglected.) The amplification factor is a constant, dependent only on the ion type, as long as the wave function varies slowly over the region of the ion core orbitals; that criterion ought to be well satisfied here, where the wave function in question is highly diffuse.

Isotropy of the g factor also implies that the ESR linewidth must be due entirely to hyperfine broadening. By using a standard formula⁶ for the second moment of the ESR line, and by using constants appropriate to I^{127} and the RES, we calculate

$$\Delta H = 3.527 \left[\sum_i (\nu_{\text{hf}i})^2 \right]^{1/2} \text{ Oe}, \quad (3)$$

where ΔH is the full width at the half-power points of the ESR line, ν_{hf} values are in megahertz, and the sum is over all surrounding I^{127} nuclei in significant contact with the F center.

From Eqs. (1), (2), and (3), ΔH can be computed as a function of η . Because the sum in (3) involves dozens of terms, the calculations were carried out on a computer. The result may be described briefly as follows: For $\eta \leq 0.7$, ΔH increases almost exactly as $\eta^{3/2}$; it then reaches a peak value for $\eta = 1.7$, and then rapidly goes to zero as $\eta \rightarrow \infty$. Using the amplification factor $A_S = 7500$ given by Seidel,⁸ the peak value is $\Delta H = 3.5$ kOe. Thus, there are two values of η that would match the experimental linewidth; one is $\eta \sim 0.3$ and the other is $\eta \sim 3$, but the larger value is unacceptable on both theoretical as well as empirical grounds. (Since the A value referred to above is not expected to be very accurate, neither is the η value extracted from ΔH alone).

By making a simultaneous fit to both $(\nu_{\text{hf}})_{\text{max}}$ and ΔH , we may extract a rather precise value of η without having to know A . That is, for η in the neighborhood indicated above, the resultant diffuse wave function will always have one or more shells of iodine nuclei near its peak. Since the wave function peaks at $\eta\rho = 1$, we may write

$$(\nu_{\text{hf}})_{\text{max}} \cong C_1 A (\eta^3/3\pi) e^{-2}. \quad (4)$$

And from the calculation of $\Delta H(\eta)$, we may extract

$$\Delta H = C_2 A \eta^{3/2}, \quad (5)$$

where $C_2 = 0.2975$ Oe. Now, from the ratio of Eqs.

(4) and (5), and by inserting the experimental values for $(\nu_{\text{hf}})_{\text{max}}$ and ΔH , we obtain $\eta = 0.50$. A value of A only 35% less than A_S is implied. In view of the many assumptions involved in the determination of A_S , the difference is not at all hard to accept.

The next step is to try to make a detailed fitting to the ENDOR spectrum. For this purpose, we may make fine adjustments in η about $\eta = 0.50$, while simultaneously adjusting A such that the correct ESR linewidth is maintained. A good fit has been obtained for $\eta = 0.515$ and $A = 5300$. The fit is illustrated in Fig. 1, where eleven values of probability density, as deduced from discrete ENDOR frequencies (encircled dots), are compared with a plot of Eq. (1) (solid line). The numbers beside each dot indicate the number of equivalent nuclei, n_s , in each shell. Since the line intensities ought to increase monotonically with n_s , it is easy to believe that the signals from the two shells containing only six nuclei each are simply buried in the overlapping tails of the much stronger adjacent lines.

We have also made a computer simulation of the ENDOR spectrum, based on the theoretical ENDOR frequencies, and with linewidths adjusted for a best fit. Each normalized line was multiplied by an intensity factor $n_s(\nu_E)_s^2 \{1 - \exp[-(\nu_{\text{hf}}/\Delta)^2]\}$, $\Delta = 9.9$ MHz, to reflect, if only crudely, expected dependence on n_s , to reflect the fact that

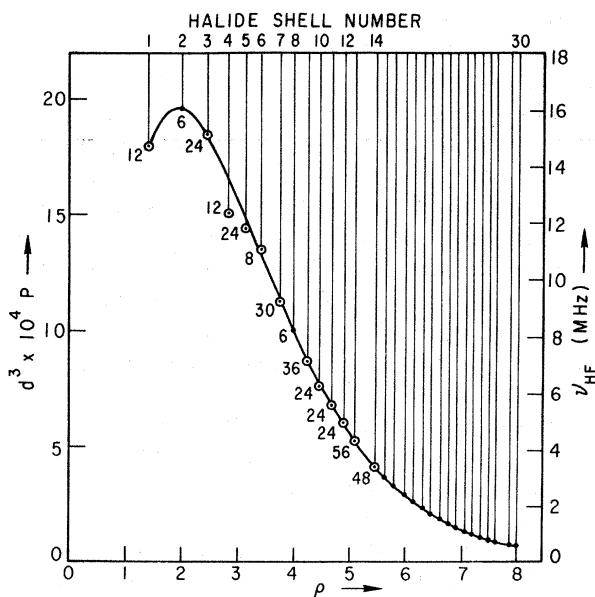


FIG. 1. Probability density $P(\rho)$ (times d^3). ρ is in units of the lattice parameter $d = 3.525$ Å. Solid curve, graph of Eq. (1) for $\eta = 0.515$. Encircled dots, experimental points (see text).

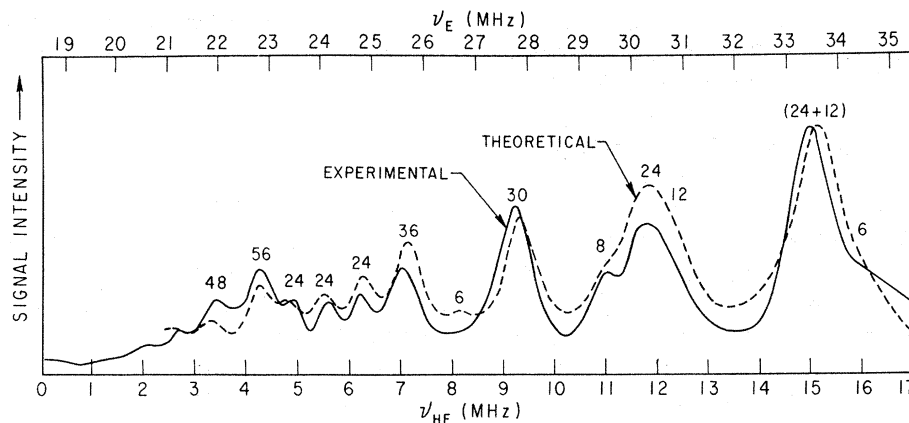


FIG. 2. Experimental ENDOR spectrum (solid curve) compared with computer simulation (dashed curve). The number beside each peak is the number n_s of equivalent nuclei in the shell associated with the peak (see text).

the probability for flipping a nuclear spin goes as $(\nu_E)^2$ for the rf intensities used, and to reflect the fact that cross-relaxation effects tend to "short-circuit" the ENDOR at low values of ν_{hf} . (This last effect is most dramatic in the optically detected ENDOR of the ground state.⁷) The best fit is shown in Fig. 2. To obtain that fit, only one frequency had to be significantly shifted from the theoretical value according to the $|2p\rangle$ distribution; this shift is indicated clearly in Fig. 1.

The deviation of the empirically measured $P(\rho)$ from the $P_p(\rho)$ of Eq. (1) probably can be explained qualitatively as follows. The potential is Coulombic only in an average sense; in detail it contains peaks and valleys. In particular, the point-ion potential contains a large peak⁸ in just the region ($\rho \sim 2.7$) where $P(\rho)$ is depressed. From this point of view, it is somewhat amazing that the simple Coulombic $|2p\rangle$ function works as well as it does.

It should be mentioned that various admixtures of $|2s\rangle$ probability density were also tried, where $P_s \propto (1 - \eta\rho)^2 \exp(-2\eta\rho)$. The mixtures were of the form $a^2 P_s + (1 - a^2) P_p$. (This form is consistent with dynamic Jahn-Teller treatment.) It was found that admixture of P_s always made the fit worse. For example, for $a^2 \geq 0.2$, and for values of η in the neighborhood of 0.5, the P_s admixture always produced a large gap between $(\nu_{hf})_{max}$ and the next lower value, in contrast to experiment. However, this failure in KI is not necessarily inconsistent with the $|s\rangle, |p\rangle$ state admixture proposed⁹ for the RES in KCl. The $|2s\rangle, |2p\rangle$ splitting in a cubic field may be significantly different in KCl and KI.

The value of η determined from this fitting is in remarkable agreement with the results of Fowler's

relaxation calculation¹⁰ on the F center in NaCl. It would be most satisfying if his calculation were repeated for the parameters specific to KI, so that comparison would not have to be by extrapolation.

The proposed wave function is consistent with the known radiative lifetime of KI at zero temperature, $\tau = 3.2 \mu\text{sec}$.¹¹ A standard calculation of the squared transition matrix element $|x|_\tau^2$ implied by τ , brackets $|x|_\tau^2$ between the values $0.0046d^2$ and $0.0072d^2$, the upper limit obtaining for no local field correction, the other with full correction. By extrapolating from Fowler's work¹⁰ to obtain an appropriate terminal-state wave function, and using the excited-state wave function proposed here, we calculate $|x|_{\text{calc}}^2 = 0.0072d^2$. The agreement with the upper bound of $|x|_\tau^2$ is probably somewhat fortuitous, since, for example, a reduction of only 7% in the mean radial extent of the ground-state wave function is required to produce a value of $|x|_{\text{calc}}^2$ equal to the lower bound of $|x|_\tau^2$.

If η/d does not change significantly from one host lattice to the next in the sequence KI, KBr, KCl, then ΔH ought to scale as the factor $A[I(I+1)]^{1/2} g_N g_e^{-1} d^{-3/2}$, where g_N is the halide nuclear g factor, and where g_e is the electronic g factor for the RES. By using the ratios of amplification factors given in Ref. 6, from $\Delta H = 575$ Oe for KI, we calculate $\Delta H \cong 284$ Oe for KBr, which compares well with the experimental value³ of 270 ± 10 Oe; making the same extrapolation to KCl, we calculate $\Delta H \cong 35$ Oe, as opposed to the experimental value³ of 55 Oe. However, if we use the lower amplification factor found here for KI, then the extrapolated KCl value becomes $\Delta H \cong 49$ Oe, in much better agreement with experiment.

It probably cannot be determined at this point whether or not the extrapolation to KCl is valid, or if in fact the RES wave function is somewhat different for KCl.

A few years ago it was generally thought that detection of ESR and ENDOR in the RES of the F center would be impossible. Yet the experiments have now been done, and interpretation of the ENDOR has proven remarkably straightforward and rather definitive. We trust that this work will form a solid cornerstone for further theoretical work on the RES. In particular, we would urge a refinement of the relaxation calculations, and an extension of Ham's treatment to include the ESR g factor and other magnetic effects.

Note added.—Following completion of this manuscript, we succeeded in detecting ENDOR of the RES in KBr for the first time. As expected, the spectrum is not resolved, but a value of $(\nu_{\text{hf}})_{\text{max}} = 11.8 \pm 0.5$ MHz for Br^{81} can be extracted from it. Again, assuming a pure $|2p\rangle$ state, and analyzing as above, we obtain $\eta \sim 0.48$ in KBr and $A \sim 3000$ for Br.

We would like to acknowledge the constant encouragement and support given this work by C. D. Jeffries. A number of conversations with W. B. Fowler have been most helpful. Finally, we are

indebted to H. Engstrom and Miss L. Pang for assistance with the computer calculations.

†Research supported in part by the U. S. Atomic Energy Commission, Report No. UCB-34P20-155.

*Present address: Bell Telephone Laboratories, Holmdel, N. J.

‡Visiting fellow from Comitato Nazionale per l'Energia Nucleare, Laboratori Nazionali de Frascati, Italy.

¹L. F. Mollenauer, S. Pan, and S. Yngvesson, *Phys. Rev. Lett.* **23**, 683 (1969).

²L. F. Mollenauer, S. Pan, and A. Winnacker, *Phys. Rev. Lett.* **26**, 1643 (1971).

³L. F. Mollenauer and S. Pan, *Phys. Rev. B* (to be published).

⁴F. S. Ham, *Phys. Rev. Lett.* **28**, 1048 (1972).

⁵W. B. Fowler, in *Physics of Color Centers*, edited by W. B. Fowler (Academic, New York, 1968), p. 85.

⁶H. Seidel, *Z. Phys.* **165**, 218 (1961); H. Seidel and H. C. Wolf, in Ref. 5.

⁷L. F. Mollenauer, A. Winnacker, and S. Pan, unpublished.

⁸J. K. Kübler and R. J. Friauf, *Phys. Rev.* **140**, A1742 (1965), or see Figs. 2-4, p. 57 in Ref. 5.

⁹L. D. Bogan and D. B. Fitchen, *Phys. Rev. B* **1**, 4122 (1970).

¹⁰W. B. Fowler, *Phys. Rev.* **135**, A1725 (1964).

¹¹H. Mahr, in Ref. 5, p. 270.

Resonance Raman Scattering in InSb near the E_1 Transition*

Peter Y. Yu† and Y. R. Shen

Department of Physics, University of California, Berkeley, California 94720, and Inorganic Materials Research Division, Lawrence Berkeley Laboratory, Berkeley, California 94720

(Received 1 May 1972)

Resonance Raman scattering in InSb near the E_1 transition has been measured at low temperatures for various different configurations with a tunable dye laser. The experimental curves show a resonance peak at an incident photon energy appreciably higher than the energy of the E_1 peak in the reflectivity spectra, contrary to the predictions of existing theories. Double resonance in the Raman tensor involving transitions in the band continuum is proposed to explain the result.

Recently, considerable theoretical¹ and experimental²⁻⁵ interest has been focused on resonance Raman scattering (RRS). However, most of the experimental investigations have so far been carried out with only a few discrete laser frequencies. Since these discrete laser frequencies are separated by 0.1 eV or more, it becomes difficult to obtain detailed information about RRS, especially for resonances which have half-widths smaller than 0.1 eV. This difficulty is overcome with the availability of tunable dye lasers.⁶ Mea-

surements of RRS using a tunable dye laser have already been reported in CdS near bound exciton lines⁷ and in Ge near the E_1 and $E_1 + \Delta_1$ transitions.⁸ This Letter is a preliminary report of a detailed study of RRS by TO and LO phonons in InSb near the E_1 transition carried out with a cw tunable dye laser. Our results indicate that in InSb the E_1 hyperbolic exciton contributes negligibly to the RRS, but rather, it is transitions involving the band continuum that are responsible for the observed resonance enhancement in the